MARCH 01 2006

On analysis of exponentially decaying pulse signals using stochastic volatility model

C. M. Chan; S. K. Tang; H. Wong

J. Acoust. Soc. Am. 119, 1519–1526 (2006)
https://doi.org/10.1121/1.2168415

On analysis of exponentially decaying pulse signals using stochastic volatility model

C. M. Chan
Hong Kong Community College, The Hong Kong Polytechnic University, Hong Kong, China

S. K. Tang
Department of Building Services Engineering, The Hong Kong Polytechnic University, Hong Kong, China

H. Wong
Department of Applied Mathematics, The Hong Kong Polytechnic University, Hong Kong, China

(Received 9 August 2005; revised 3 January 2006; accepted 4 January 2006)

A stochastic volatility model incorporating the exponential power distributions is adopted in the present study to analyze exponentially decaying pulses in the presence of background noises of various magnitudes. The discussions are focused on its effectiveness in the determination of the instant of the pulse initiation and the decay constant. The results are compared with those obtained by the conventional short-time Fourier transform. It is found that the present stochastic volatility model can retrieve the instant of the pulse initiation and the decay constant within engineering tolerance even when the noise is slightly stronger that the pulse amplitude. Its performance is substantially better than that of the Fourier transform when the frequency of the decay pulse fluctuates. © *2006 Acoustical Society of America.* [DOI: 10.1121/1.2168415]

PACS number(s): 43.60.Uv, 43.60.Jn, 43.60.Cg, 43.60.Hj [EJS] Pages: 1519–1526

I. INTRODUCTION

Quick and accurate signal detection is one of the important research areas in acoustics and building services engineering. Modern buildings are usually heavily serviced and the signals from the services equipments, both the acoustic and vibration signals, are commonly used in the equipment health monitoring processes.[1] Since most of these signals are not stationary, signal processing techniques, such as the short-time Fourier transform (STFT)[2] and the wavelet transforms (WTs),[3] have been proposed and tested in the past few decades. The more efficient extraction of localized signal information using the WT has attracted the interests of many engineers and scientists, especially in the detection of gear faults (for instance, Ref. 4). Pulses and their decays have also been used to measure the energy dissipation of a system. Typical examples are the estimation of room sound absorption and structural damping using reverberation time measurements.[5,6] Under a sufficiently diffused condition, this kind of pulse decay is theoretically an exponential function of time.

In reality, there are background noises, and thus the signal-to-noise ratios (S/N) are of prime importance in the resolution of changes in a signal. For the reverberation time measurement in a noisy environment, the maximum length sequence[7] gives satisfactory results provided that the signal is not too weak when compared to the noise. At high S/N, both the STFT and the WT perform well in the measurement of the decay constant.[8] Wong *et al.*[9] has investigated the use of the WT in locating jumps in a time series when the magnitudes of the jumps are significant.

Conventional parametric models, such as the autoregressive moving averages,[10] have also been used to analyze nonstationary time series. However, these methods do not allow the conditional variances of the data to be a deterministic function of the past observations. This is not realistic in practice, especially when the responses of an excited system are concerned.

A sharp pulse followed by a decay embedded in a random noise, provided that its magnitude is not too weak when compared to that of the noise, will create a relatively higher volatility in the signal fluctuations at the instant the pulse is introduced. A more advanced parametric model, namely the stochastic volatility (SV) models,[11] which have been widely used in modeling time series volatilities, are expected to be useful in the modeling of the above-mentioned pulse signal. The properties of these models and their formulation in the present study will be discussed in the next section. Recently, these models have been used together with efficient Bayesian computational technique in analyzing time series in economic studies (for instance, Ref. 12). However, they are rarely applied, at least to the knowledge of the authors, to deal with engineering problems, though some sort of Bayesian model selection has been considered in the study of geoacoustic signal.[13]

In this paper, the performance of a specific SV model on retrieving the properties of exponentially decaying pulses in the presence of random noises will be presented. It is hoped that the results will provide useful information for the future enhancement of signal detection and machine diagnosis.

II. STOCHASTIC VOLATILITY MODEL

The SV model formulates the volatility by a numerical process which allows the latter to vary stochastically.[11] It involves the use of a statistical distribution so chosen to fit the time series/signal to be analyzed. Both the Guassian distribution and the Student t distribution have been employed

in determining outlying observations in financial time series.[14,15] Recently, Choy and his co-workers have investigated the properties of the SV model which incorporates the exponential power (EP) distributions.[14–16] In their studies, the EP distribution is expressed as scale mixtures representation, which can highly decrease the computational time in the numerical simulation study. Also, the mixing parameters in the representation can be used to identify the extreme data very accurately. Therefore, the EP distributions are adopted in the present study. A brief introduction of the SV model is given in the Appendix.

A. Exponential power distributions

The exponential power family of distributions provides both heavier- and/or lighter-tailed distributions than the normal Guassian one. Let $\{y\}$ be the data set, θ its mean, σ its scale parameter, and $\beta \in (0,2]$ the kurtosis parameter that controls the thickness of the tails. The density function of the EP distribution $\mathrm{EP}(y,\theta,\sigma,\beta)$ is given by[17]

$$\mathrm{EP}(y|\theta,\sigma,\beta) = \frac{1}{2^{(1+\beta/2)}\Gamma(1+\beta/2)\sigma} \exp\left(-\frac{1}{2}\left|\frac{y-\theta}{\sigma}\right|^{2/\beta}\right), \tag{1}$$

where Γ is the gamma function. The corresponding mean and variance are equal to θ and $2^{\beta}\Gamma(3\beta/2)/[\sigma^2\Gamma(\beta/2)]$, respectively. The EP distribution has been studied thoroughly by a number of researchers for statistical modeling and Bayesian robustness (for instance, Choy and Walker[18] and Choy and Chan[15]). Choy and Smith[16] adopted the normal scale mixtures property of the EP density for Bayesian inference using Markov chain Monte Carlo methods with $1<\beta \leqslant 2$. Recently, Walker and Gutierrez-Pena[19] discovered the following uniform scale mixtures representation for the EP density:

$$\mathrm{EP}(y|\theta,\sigma,\beta) = \int_0^{\infty} U(y|\theta-\sigma u^{0.5\beta}, \theta+\sigma u^{0.5\beta}) \times G(u|1+0.5\beta,0.5)\, du, \tag{2}$$

where $U(y|a,b)$ is the uniform density function defined on the interval (a,b) and $G(y|c,d)$ is the gamma density function with mean c/d. This representation is valid for the entire range of β and also allows rewriting the EP distribution into the following hierarchical form:

$$y|u \sim U(\theta-\sigma u^{0.5\beta}, \theta+\sigma u^{0.5\beta}) \quad \text{and} \quad u \sim G(1+0.5\beta,0.5), \tag{3}$$

where u is referred to as the mixing parameter of the uniform scale mixtures representation. It should be noted that the normal and the Laplace distributions are special cases of the EP family with $\beta=1$ and 2, respectively.

B. Bayesian EP SV model

In this paper, the family of EP distributions is considered as a generalization of the normal family to model the signal data. This family provides both leoptkutic and platykurtic shapes of distributions which the normal, Student t, and stable families cannot offer. From a practical point of view, the EP distribution is believed to be appropriate to model certain types of data and it is worthwhile to develop efficient methods for statistical analysis. A Gibbs sampling approach using the uniform scale mixtures is discussed in Sec. III.

The usual choice of the normal distribution for the white noise ε_t of the SV model is replaced by the EP distribution with known kurtosis parameter β:

$$y_t|h_t \sim \mathrm{EP}(0, e^{0.5h_t}, \beta), \tag{4}$$

where t is the index and $t=1,2,\ldots,n$. h is the log volatility. Expression (4) can be rewritten into the following hierarchical form:

$$y_t|h_t,u_t \sim U(-e^{0.5h_t}u_t^{0.5\beta}, e^{0.5h_t}u_t^{0.5\beta}) \quad \text{and} \quad u_t \sim G(1+0.5\beta,0.5), \tag{5}$$

where u is the mixing parameter of the SV model. Normality assumption is still valid for the conditional and marginal distributions of h in the present study:

$$h_t|h_{t-1},\phi,\sigma^2 \sim N(\phi h_{t-1},\sigma^2) \quad \text{and} \quad h_t|\phi,\sigma^2 \sim N(0,\sigma^2/(1-\phi^2)), \tag{6}$$

where $N(0,\alpha)$ is the normal distribution with mean 0 and standard deviation α, and ϕ is the persistence parameter. The above SV model with EP white noise and normal log volatility is referred as the EP-N SV model. In order to complete a full Bayesian framework for the SV model, the following are assigned prior to other model parameters:

$$\sigma^2 \sim G_{inv}(a_\sigma,b_\sigma) \quad \text{and} \quad \phi+1 \sim 2Be(a_\phi,b_\phi), \tag{7}$$

where $Be(a,b)$ is the beta distribution with mean $a/(a+b)$, G_{inv} is the inverse gamma distribution, and a_σ, b_σ, a_ϕ, and b_ϕ are prespecified constants. The prior distribution for ϕ is a shifted beta distribution with density

$$p(\phi) \propto (1+\phi)^{a_\phi-1}(1-\phi)^{b_\phi-1}, \quad |\phi|<1. \tag{8}$$

III. GIBBS SAMPLER FOR EP-N SV MODELS

The simulation-based Gibbs sampling approach[20] is one of the standard methods for carrying out statistical analysis of complicated Bayesian models. The Gibbs sampler allows us to study posterior characteristics via a sequence of iteratively simulated values drawn from a system of full conditional distributions. The efficiency of the Gibbs sampler can be substantially increased if the required samples are drawn from distributions of some standard forms. Gibbs sampling has also been used in underwater acoustic application.[21]

The joint distribution of $\vec{y}=(y_1,y_2,\ldots,y_n)$, $\vec{h}=(h_1,h_2,\ldots,h_n)$, $\vec{u}=(u_1,u_2,\ldots,u_n)$, ϕ, and σ^2 is given by

$$p(\vec{y},\vec{h},\vec{u},\phi,\sigma^2) = \prod_{t=1}^{n} p(y_t|h_t,u_t)p(h_1|\phi,\sigma^2)p(\vec{u})p(\phi)p(\sigma^2). \tag{9}$$

Then, the Gibbs sampling scheme performs successive random variate generation from the following conditional distri-

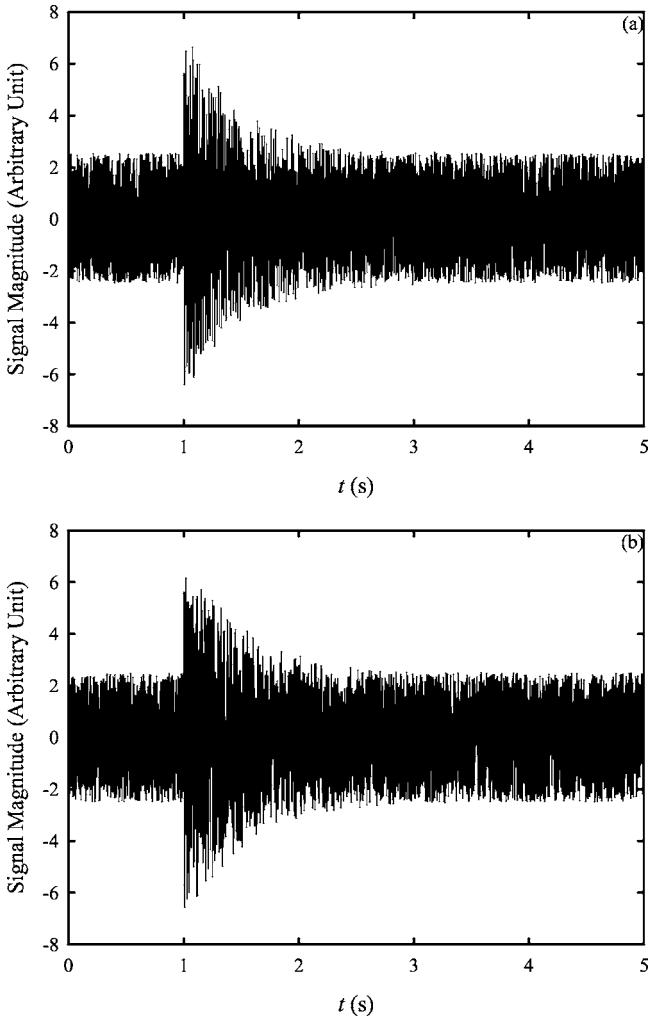

FIG. 1. Examples of exponentially decaying signals with $S/N=10$ dB. (a) Constant f. (b) Time varying f.

butions. The duration of the Gibbs sampler computation varies from a few minutes to about 25 min on a Pentium V personal computer, depending on the kurtosis parameter of the EP distribution. The number of iterations adopted is 12 000 with the first 2000 iterations as the burn-in period. In the foregoing discussions, $\vec{h}_{-t}=(h_1,\ldots,h_{t-1},h_{t+1},\ldots,h_n)$ and $\vec{u}_{-t}=(u_1,\ldots,u_{t-1},u_{t+1},\ldots,u_n)$.

A. Full conditional densities of *h*

Full conditional density of h is given by

$$p(h_t|\vec{y},\vec{h}_{-t},\vec{u},\phi,\sigma^2) \propto p(y_t|h_t,u_t)p(h_t|h_{t-1},u_t,\phi,\sigma^2)p(h_{t+1}|h_t,u_{t+1},\phi,\sigma^2). \tag{10}$$

One can then show that these full conditional distributions are truncated normal of the form

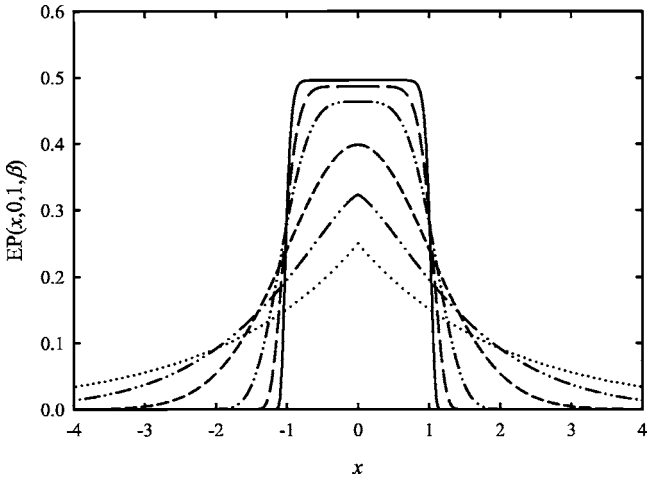

FIG. 2. Effects of β on the shape of an EP distribution. ———: $\beta=0.1$; – – –: $\beta=0.25$; –·–: $\beta=0.5$;- - -:$\beta=1$; –·· –: $\beta=1.5$; ···: $\beta=2$.

$$h_t|\vec{y},\vec{h}_{-t},\vec{u},\phi,\sigma^2 \sim \begin{cases} N(\phi h_{t+1}-\sigma^2/2,\sigma^2), & t=1, \\ N\left(\dfrac{\phi(h_{t-1}+h_{t+1})-\sigma^2/2}{1+\phi^2},\dfrac{\sigma^2}{1+\phi^2}\right), & 2\leqslant t\leqslant n-1, \\ N(\phi h_{t-1}-\sigma^2/2,\sigma^2), & t=n, \end{cases} \tag{11}$$

subject to $h_t>\ln y_t^2-\ln\beta^2-\alpha\ln u_t$. The algorithm proposed by Robert[22] is an efficient method for generating random variates from the truncated normal distribution.

B. Full conditional densities of *u* and σ^2

By representing the EP density into a uniform scale mixtures form, one can show that the full conditional distribution of the mixing parameter u is a truncated exponential distribution of the form

$$u_t|\vec{y},\vec{h},\vec{u}_{-t},\phi,\sigma^2 \sim \exp(u|0.5)=0.5e^{-0.5u}, \tag{12}$$

subject to the condition

$$u_t^{\beta}>\frac{y_t^2}{\beta^2}e^{-h_t}. \tag{13}$$

The inversion method can be used to sample random variates from the truncated exponential distribution. For σ^2, the use of conjugate prior leads to an inverse gamma full conditional distribution and σ^2 can then be directly sampled from

$$\sigma^2|\vec{y},\vec{h},\vec{u},\phi \sim G_{inv}\left(a_\sigma+\frac{n}{2},b_\sigma+\frac{1}{2}\left((1-\phi^2)h_1^2+\sum_{t=2}^{n}(h_t-\phi h_{t-1})^2\right)\right). \tag{14}$$

C. Full conditional densities of ϕ

The full conditional density of ϕ is given by

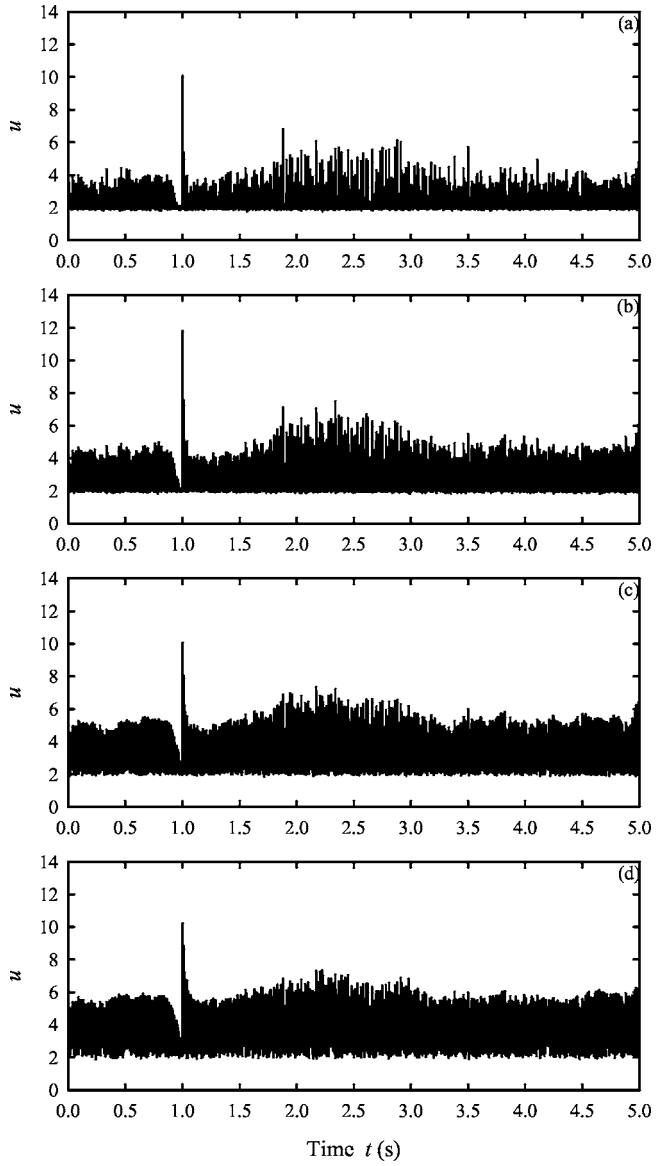

FIG. 3. Effects of β on the time variation of the mixing parameter u. (a) β=0.25; (b) β=0.75; (c) β=1.5; (d) β=2.0. S/N=10 dB.

$$p(\phi|\vec{y},\vec{h},\vec{u},\sigma^2) \propto p(h_1|\phi,\sigma^2)\prod_{t=1}^{n} p(h_t|h_{t-1},\phi,\sigma^2)p(\phi). \tag{15}$$

It can easily be verified that $\Pi_{t=2}^{n} p(h_t|h_{t-1},\phi,\sigma^2)$ is proportional to a normal density of ϕ with mean μ_ϕ and variance σ_ϕ^2 where

$$\mu_\phi = \frac{\sum_{t=1}^{n-1} h_t h_{t+1}}{\sum_{t=1}^{n-1} h_t^2} \quad \text{and} \quad \sigma_\phi^2 = \frac{\sigma^2}{\sum_{t=1}^{n-1} h_t^2}. \tag{16}$$

One can express the full conditional density by a product of a truncated normal function and a shifted beta density function:

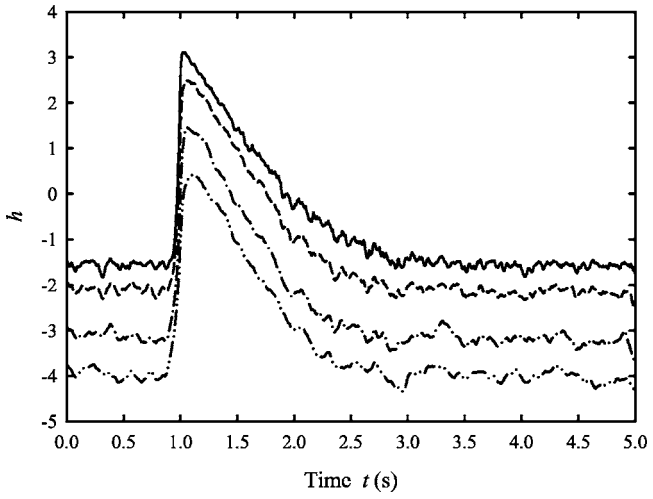

FIG. 4. Effects of β on the time variation of the log-volatility h. ———: β=0.25; - - -:β=0.75; –·–: β=1.5; –·· –: β=2.0. S/N=10 dB.

$$p(\phi|\vec{y},\vec{h},\vec{u},\sigma^2) \propto N\left(\frac{\sum_{t=1}^{n-1} h_t h_{t+1}}{\sum_{t=2}^{n-1} h_t^2}, \frac{\sigma^2}{\sum_{t=2}^{n-1} h_t^2}\right) \times (1+\phi)^{a_\phi - 1/2}(1-\phi)^{b_\phi - 1/2} \tag{17}$$

for $|\phi<1|$. Sampling random variates from this full conditional density can be done easily by using the Metropolis-Hastings method.[23]

IV. NUMERICAL EXAMPLES

An exponentially decaying harmonic wave is chosen for the illustrations. This kind of signal can be regarded as the simplest (but important) signal in acoustics and vibration studies. The noise signals $n(\tau)$, where τ denotes measurement time, used in the foregoing illustrations are white noises with zero mean values and are Gaussian distributed fluctuations. The combined signal $y(\tau)$ is

$$y(\tau) = s(\tau) + n(\tau), \tag{18}$$

where $s(\tau)$ contains the pulses. The S/N in dB is defined as

$$\text{S/N} = 10\log_{10}(|s|_{\max}/|n|_{\max}). \tag{19}$$

Suppose the pulse is initiated at $\tau=\tau_o$ and let η be the decay constant; the signal $y(\tau)$ is

$$y(\tau) = e^{-\eta(\tau-\tau_o)}\cos(2\pi f(\tau-\tau_o))\mathrm{H}(\tau-\tau_o) + n(\tau), \tag{20}$$

where H denotes the Heavside step function and f is the frequency of the harmonic wave. The present investigation focuses on the determination of the instant of the pulse initiation and the decay constant η. The S/N ranges from $+\infty$ to -10 dB. Without loss of generality, η is fixed at 2 and f is normally set at 50 Hz, but is allowed to have a narrow ±10% time fluctuation in some cases discussed later. τ_o =1 s throughout the present investigation. Figures 1(a) and 1(b) illustrate the hypothetical signals with S/N =3 dB with constant f(≡50 Hz) and time varying f(=50 Hz+10% time fluctuation), respectively. One can notice that the signal with fluctuating f does not show a clearly exponential decay feature [Fig. 1(b)].

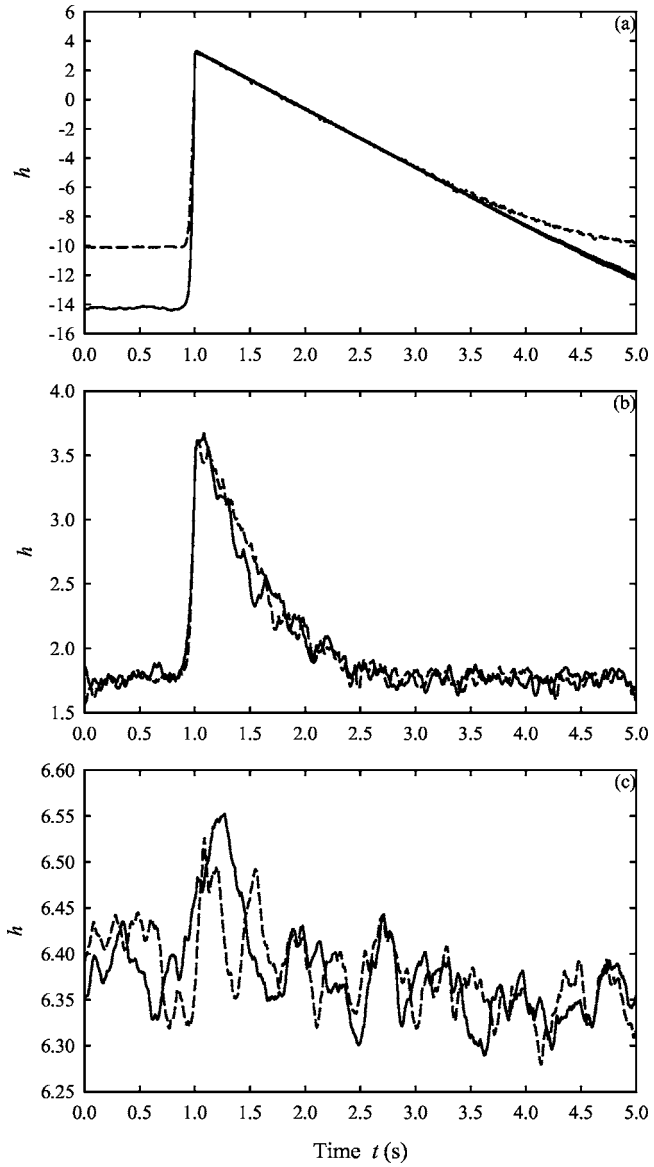

FIG. 5. Time variations of h at increased noise magnitude with $\beta=0.1$. (a) S/N=$+\infty$ dB; (b) S/N=3 dB; (c) S/N=−7 dB———: constant f; – –: time varying f.

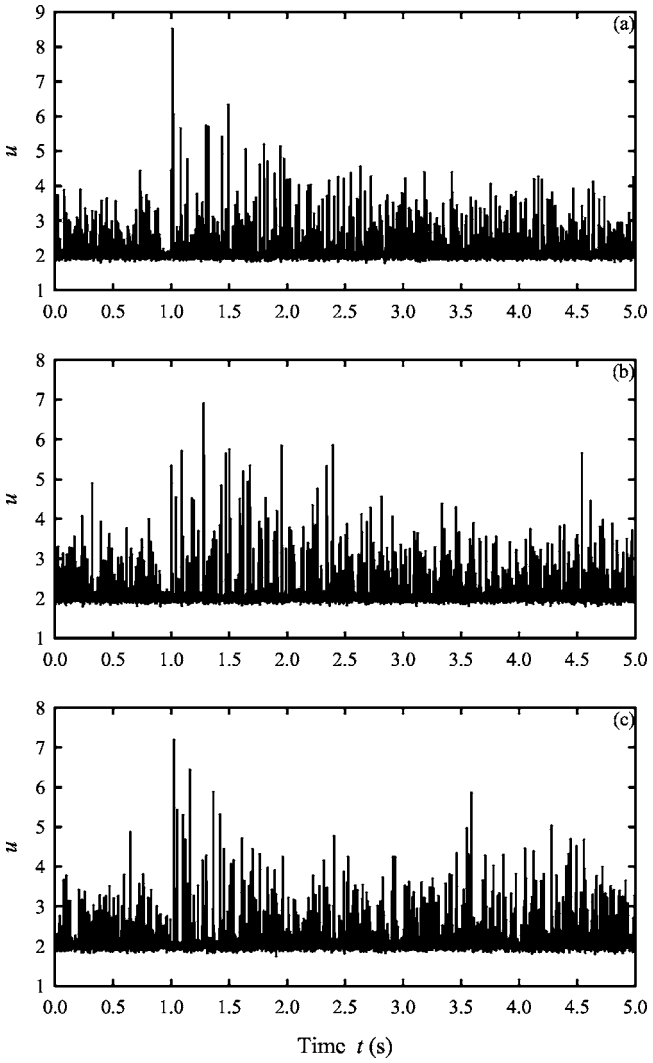

FIG. 6. Time variations of u at increased noise magnitude with $\beta=0.1$. (a) S/N=3 dB; (b) S/N=0 dB; (c) S/N=−7 dB.

The parameter β in the SV model determines the shapes of the EP distributions and thus has significant impact on the modeling of the decaying signal by the SV model. The EP distributions at various β are given in Fig. 2. A large β gives rise to a thick tail of the distribution and is in general not good for detecting changes as a thick tail distribution tends to down-weight the extreme values and thus affect the detection of pulses in the presence of a random noise.

Two parameters are important in the SV model. They are the mixing parameter u and the log volatility h. The former illustrates fluctuation and thus should be able to suggest the instants of rapid changes in a signal. The latter should follow the shapes of the decaying pulses. In the analysis of a decaying pulse, these two parameters should not be considered in isolation.

A. Constant *f*

Figure 3 shows the time variations of u at different β for S/N=10 dB. The signal is considerably stronger than the background noise in this case. One can notice a prominent sharp peak within a continuous background spikes in each case illustrated. This peak appears around the instant of the pulse initiation. In fact, the magnitudes of the background spikes before the peak, which are due to the background Gaussian noise, relative to that of the sharp peak increase with increasing β. It is found from a closer look at the data at around $\tau=1$ s that the magnitudes of the spikes continue to decrease when τ increases towards 1 s as shown in Fig. 3(a) with S/N=10 dB and $\beta=0.25$. A clear reversal is observed

TABLE I. Estimated τ_o and η (constant f).

S/N (dB)	SV model		STFT
	τ_o (S)	η (s^{-1})	η (s^{-1})
$+\infty$	1.000	2.00	2.00
10	1.000	2.05	2.05
3	1.000	2.16	1.81
0	1.001	2.42	1.58
−3	1.002	2.36	1.30
−7	1.022	⋯	⋯

TABLE II. Estimated τ_o and η (fluctuating f).

	SV model		STFT	
S/N (dB)	τ_o (S)	η (s^{-1})	t_o (s)	η (s^{-1})
∞	1.000	2.00	0.96	2.53
10	1.000	2.04	0.96	2.83
3	1.000	2.30	⋯	1.85
0	1.010	2.48	⋯	1.10
−3	1.001	2.37	⋯	⋯
−7	⋯	⋯	⋯	⋯

at $\tau=1$ s. A similar phenomenon is also observed at other values of β investigated in the present study under this signal-to-noise ratio.

The time variations of the log volatility h for S/N $=10$ dB with various β are presented in Fig. 4. The result obtained with $\beta=0.1$ resembles very much that with $\beta=0.25$ and thus is not presented. The patterns of the h variations in general follow a linear decay but the increase in β appears to have smoothed the pulse identity. The linear decay also becomes less obvious as β increases. Therefore, only results at $\beta=0.1$ will be presented in the foregoing discussions.

A decrease in the S/N results in a rocky decay of h and the exponential decay becomes slightly untraceable at S/N $=-7$ dB though a decaying pulse is still suggested by the time variation of h (Fig. 5). However, a clear reversal in u at $\tau\sim 1$ s remains prominent even up to a S/N of 0 dB and some indications of an abrupt signal jump are still observable at S/N$=-7$ dB (Fig. 6). One should note that the instant of the peak u does not necessarily collapse with that of the pulse initiation. The focus should be on the instant of the reversal. It should also be noted that the magnitude of the u peak does not carry much meaning in engineering applications. Table I summarizes the instant of the u reversal under different S/Ns with $\beta=0.1$. Though one can anticipate ambiguity in determining the instant of this major u reversal at strong background noise magnitude and thus the error in locating the instant of the pulse initiation, the prominent sharp rise of u, such as that observed in Fig. 6(c), indicates together with the variation of h that some important changes are embedded in a random signal. This shows the versatility of the present SV model in detecting changes.

Apart from detecting the instant of the pulse initiation, the determination of the decay constant is also an important task in the signal analysis.[8] The method shown in the Appendix is adopted to minimize the effects of the background noise in the process. The average h for the background noise can be obtained using 800 data points starting from $\tau=0$ s. Data points close to the major u reversal should be avoided. The patterns of h variations after the background noise correction are very similar to those of the impulse decays inside rooms and thus are not presented. The decay constant η's estimated under different S/Ns are shown in Table I. η's from the SV model are obtained using the 1000 data points after the major u reversal and the correlation coefficients R^2 of the regression are in general greater than 0.9 for S/N$\geqslant -3$ dB. The corresponding values obtained from the STFT with a frequency resolution of 3.9 Hz and 60% data overlapping are also presented in Table I for the sake of comparison. Allowing for error in the estimation of the slopes of the decay curves, the two sets of results are comparable. However, the STFT is not able to provide the time resolution one can obtain from the present SV model unless the frequency resolution is lowered to 40 Hz and the S/N is high. Thus, the STFT is not suitable for the determination of τ_o.

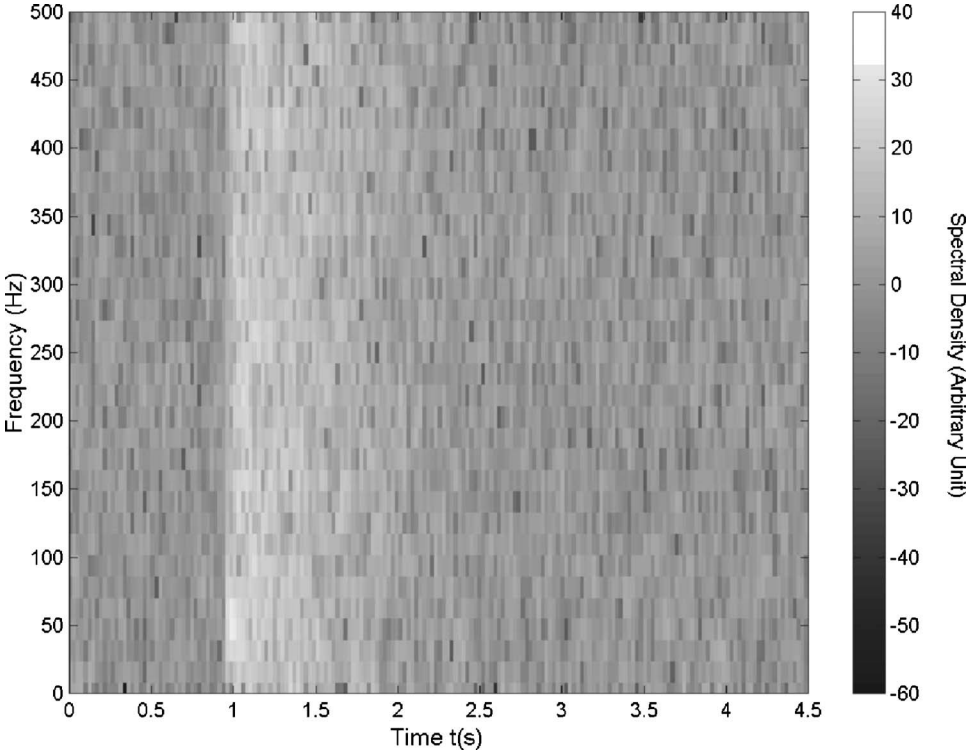

FIG. 7. Time-frequency plot of an exponential decaying signal with time varying f. S/N$=10$ dB, frequency resolution: 15.6 Hz.

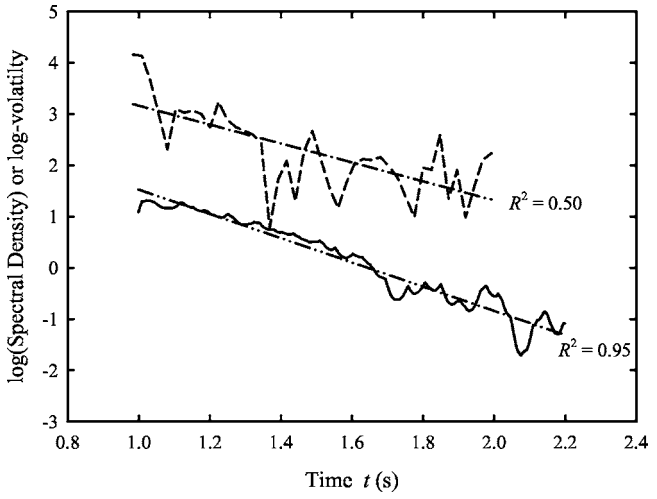

FIG. 8. Decay curves with time varying f at S/N=3 dB———: log-volatility $h(\beta=0.1)$–·–·–: regression line for h; – –:log (spectral density); –·–: regression line for log (spectral density).

B. Time varying *f*

The introduction of a ±10% Gaussian fluctuation in f does not greatly affect the pattern of the time varying mixing parameter u. A major reversal of u can again be observed at the instant close or equal to τ_o when S/N>-3 dB, but such reversal becomes ambiguous when S/N is further decreased (not presented here). The fluctuation in f does increase the log volatility h when the background noise is strong relative to the signal as shown in Fig. 5. The τ_o and η determined from the present SV model with EP distribution having $\beta=0.1$ are tabulated in Table II. The randomness in f does not produces observable deterioration of the SV model performance, except that the error in locating τ_o becomes slightly higher than that in the constant f case when S/N drops below 0 dB.

The randomness in f, however, results in a broadband time-frequency distribution as computed by the STFT (Fig. 7). In order to cover the range of the frequency fluctuation, the frequency resolution here is taken to be 15.6 Hz. Sixty percent data overlapping is again adopted in the STFT and the time resolution is 0.024 s. One can notice from Table II that the STFT does not provide reliable estimation of η. The ambiguity of τ_o determination is high when S/N is less than 3 dB. Though η is estimated to be 1.85 by STFT at S/N=3 dB, the actual decay curve is problematic as shown in Fig. 8 (all corrected for background noise). The linear decay is not so reflected by the STFT, while that obtained from the present SV model is still acceptable. Reasonably good linear regression between h and τ is also obtained at S/N=0 and −3 dB (not shown here), but the STFT is unable to reveal a decay trend when S/N decreases below 0 dB.

V. CONCLUSIONS

A stochastic volatility model incorporating the exponential power distribution is used in the present study to capture the initiation and decay of exponentially decaying signals in the presence of random background noises. Its performance is compared with that of the short-time Fourier analysis.

When the pulse is a decaying harmonic wave of constant frequency, the accuracy of decay constant estimation using the present stochastic volatility model is very good when the signal-to-noise ratio is not less than 3 dB. Such accuracy deteriorates as the signal-to-noise ratio decreases, but it is still comparable to that of the short-time-Fourier transform. The present model is able to detect the instant of the pulse initiation even up to a signal-to-noise ratio of −7 dB within engineering tolerance. The short-time Fourier transform does not provide a comparable time resolution for such detection unless the frequency resolution is scarified and the signal-to-noise ratio is high.

The introduction of a time varying frequency (±10%) does not produce significant effect on the performance of the stochastic volatility model, though it raises up the volatility when the background noise is relatively strong, making the detection of the pulse difficult once the signal-to-noise ratio drops below 0 dB. However, the performance of the short-time Fourier transform is substantially worsened even in the absence of the background noise.

ACKNOWLEDGMENT

CMC is supported by a staff development porgramme of the Hong Kong Community College, The Hong Kong Polytechnic University.

APPENDIX: SV MODELING AND DECAY CONSTANT ESTIMATION

In the present study, a hypothetical signal y made up of an exponential decaying signal d initiated at $\tau=\tau_o(>0)$ and a continuous white noise (normally distributed) n is considered. The SV model suggests[11]

$$y = d + n = H_t^{1/2}\varepsilon_t, \tag{A1}$$

where ε_t is a time fluctuating white noise and H_t the volatility. Suppose one can find $d=H_{d,t}^{1/2}\varepsilon_t$ (no noise) and $n=H_{n,t}^{1/2}\varepsilon_t$, one then have the following approximate relationship.

$$H_t^{1/2} = H_{d,t}^{1/2} + H_{n,t}^{1/2}. \tag{A2}$$

Let $h_t=\log H_t$, $h_{d,t}=\log H_{d,t}$ and $h_{n,t}=\log H_{n,t}$, one can then find

$$h_{d,t} = 2\log(e^{h_t/2} - e^{h_{n,t}/2}). \tag{A3}$$

At $\tau>\tau_o$ and excluding the sinusoidal time fluctuation, one obtains $|d| \sim Ae^{-\alpha(\tau-\tau_o)}$ and $H_{d,t}^{1/2} \sim Ae^{\alpha\tau_o}e^{\alpha\tau}$ so that $h_{d,t}=\log H_{d,t}=-2\alpha\tau+2\log(Ae^{\alpha\tau_o})$, and

$$\log(Ae^{\alpha\tau_o}) - \alpha\tau = \log(e^{h_t/2} - e^{h_{n,t}/2}). \tag{A4}$$

Since n is normally distributed and thus can be treated as ε_t multiplied by a constant, it is straight-forward to conclude that

$$n = A(\mathrm{S/N})\varepsilon_t \Rightarrow e^{h_{n,t}/2} \sim A \times \mathrm{S/N}. \tag{A5}$$

One can normalize y by A such that $A=1$ in the above derivation. $h_{n,t}$ can be obtained from the data at $\tau<\tau_o$. Usually, an average from less than 400 points is good enough to get a reliable estimate of $h_{n,t}$ when S/N$\geqslant 0$.

[1]R. B. Randall, *Frequency Analysis* (Brüel & Kjær, Nærum, Denmark, 1987).
[2]C. H. Hodges, J. Power, and J. Woodhouse, "The use of sonogram in structural acoustics and an application to the vibrations of cylindrical shells," J. Sound Vib. **101**, 203–218 (1985).
[3]I. Daubechies, "The wavelet transform, time-frequency localization and signal analysis," IEEE Trans. Inf. Theory **36**, 961–1005 (1990).
[4]P. D. McFadden and W. J. Wang, "Early detection of gear failure by vibration analysis—I. Calculation of the time-frequency distribution," Mech. Syst. Signal Process. **7**, 193–203 (1993).
[5]H. Kuttruff, *Room Acoustics* (E & FN Spon, New York, 2000).
[6]M. Heckl, "Measurement of absorption coefficients on plates," J. Acoust. Soc. Am. **34**, 803–808 (1962).
[7]M. Vorländer and M. Kob, "Practical aspects of MLS measurements in building acoustics," Appl. Acoust. **52**, 239–258 (1997).
[8]S. K. Tang, "On the time-frequency analysis of signals that decay exponentially with time," J. Sound Vib. **234**, 241–258 (2000).
[9]H. Wong, W. C. Ip, and Y. Li, "Detection of jumps by wavelets in a heteroscedastic autogressive model," Stat. Probab. Lett. **52**, 365–372 (2001).
[10]G. E. P. Box and G. M. Jenkins, *Time Series Analysis Forecasting and Control*, 2nd ed. (Holden-Day, San Francisco, 1976).
[11]S. J. Taylor, "Modelling stochastic volatility," Math. Finance **4**, 183–204 (1994).
[12]E. Jacquier, N. G. Polson, and P. E. Rossi, "Bayesian analysis of stochastic volatility models (with discussion)," J. Bus. Econ. Stat. **12**, 371–417 (1994).
[13]D. J. Battle, P. Gerstoft, W. S. Hodgkiss, and W. A. Kuperman, "Bayesian model selection applied to self-noise geoacoustic inversion," J. Acoust. Soc. Am. **116**, 2043–2056 (2005).
[14]S. T. B. Choy and C. M. Chan, "Scale mixtures distributions in insurance applications," Austin Bull. **33**, 93–104 (**2003**).
[15]S. T. B. Choy and C. M. Chan, "Bayesian student-*t* stochastic volatility models via two-stage mixtures representation," 20th International Workshop on Statistical Modelling. Sydney, Australia, 10–15 July 2005.
[16]S. T. B. Choy and A. F. M. Smith, "Hierarchical models with scale mixtures of normal distribution," TEST **6**, 205–211 (1997).
[17]G. E. P. Box and G. C. Tiao, *Bayesian Inference in Statistical Analysis* (Wiley, New York, 1992).
[18]S. T. B. Choy and S. G. Walker, "The extended exponential power distribution and Bayesian robustness," Stat. Probab. Lett. **65**, 227–232 (2003).
[19]S. G. Walker and E. Gutierrez-Pena, in *Bayesian Statistics* (Oxford U. P., Oxford, 1999), Vol. **6**, pp. 685–710.
[20]A. E. Gelfand, S. E. Hills, A. Racine-Poon, and A. F. M. Smith, "Illustration of Bayesian inference in normal modes using Gibbs sampling," J. Am. Stat. Assoc. **85**, 972–985 (1990).
[21]Z. H. Michalopoulou and M. Picarelli, "Gibbs sampling for time-delay and amplitude estimation in underwater acoustics," J. Acoust. Soc. Am. **117**, 799–808 (2005).
[22]C. P. Robert, "Simulation of truncated normal variables," Stat. Comput. **5**, 121–125 (1995).
[23]S. Kim, N. Shephard, and S. Chib, "Stochastic volatility: Likelihood inference and comparison with ARCH models," Metalloberflache **65**, 361–393 (1998).